CrystEngComm

Accepted Manuscript

ROYAL SOCIETY OF CHEMISTRY

www.rsc.org/crystengcomm

CrystEngComm RSCPublishing

ARTICLE

Ionothermal effects on low-dimensionality uranyl compounds using task specific ionic liquids

Cite this: DOI: 10.1039/x0xx00000x

P. A. Smith[a] and P. C. Burns[*a,b]

Received 00th January 2012,
Accepted 00th January 2012

DOI: 10.1039/x0xx00000x

www.rsc.org/

Ionothermal methods were employed in the synthesis of two novel uranyl coordination compounds: $[C_5H_6N]_2$ $[UO_2(C_7H_7SO_3)_4(H_2O)]$ (**1**) and $UO_2(HAsO_4)(NC_5H_{11}O_2)$ (**2**), using pyridinium and betainium class ionic liquids. Results show novel ionic liquid incorporation and uranyl structural topologies, providing insight into the development of low-dimensionality uranyl complexes beyond traditional hydrothermal methods.

Introduction

Our understanding of the solid-state chemistry of $(UO_2)^{2+}$ uranyl compounds has benefited greatly from crystallographic studies of several hundred mineral and synthetic compounds over the past two decades. Structural hierarchies have emerged that probe the topologies of structural units and the roles of interstitial constituents, and that serve to highlight the importance of H_2O and H-bonding in many of these compounds.[1] Uranyl minerals usually contain OH^- and/or H_2O because they form in relatively low-temperature moist geochemical environments. Hydrothermal methods, precipitation from aqueous solution at room temperature, and diffusion of nutrients into silica hydrogels have most commonly been used to prepare novel uranyl compounds, which almost invariably incorporate H_2O as well. Synthesis at high temperatures in the absence of water, either from melts or flux-based systems, result in anhydrous compounds that often depart significantly from topological trends typical of lower-temperature compounds.[2,3] Water in uranyl minerals and synthetic compounds usually occurs in interstitial complexes, and because of the compliant nature of its associated H-bond networks, relationships between the topologies of the structural units and the interstitial complexes remain obscure. We seek to gain better insight into such relationships by synthesis of uranyl compounds at relatively low temperature in the absence of excess water by ionothermal reactions.[4]

Ionic liquids (ILs) are a versatile class of salts that melt below 100 ºC. There are many different classes of ionic liquids and a plethora of conceivable IL combinations. By varying the means of functionalization, one can produce *Task Specific* ionic liquids (TSILs). These functionalized ILs lend themselves favorably as a non-innocent solvent to a wide array of potentially specific uses, such as alternative electrolytes in electrochemical applications, as green solvents, as solvent in catalytic applications and biocatalysis, and as templating agents for inorganic applications ranging from synthesizing nanomaterials to zeolites.[5-11]

Traditional ionic liquid systems are typified by their use of poorly coordinating anions (i.e. BF_4^-, PF_6^-, and Tf_2N^-), and as such are typically poor solvents for use with metal oxides and salts.[12,13] Introduction of coordinating anions, typically via carboxyl functionalization, provides a means of greatly increasing uranyl oxide and uranyl salt solubilities. Traditional IL systems are classified as either protic or aprotic, with the former distinguished from the latter by a lack of charge permanency at the cation center; in particular, the cation usually exists in some equilibrium with the neutral species. The use of either, or even a dication species composed of both protic and aprotic centers, provides an even greater deal of chemical flexibility and means to meet charge-balancing constraints in coordination chemistry.[14]

The majority of uranyl-IL systems studied over the past couple of decades have focused on low dimensionality species: monomeric and dimeric, mainly because of relevance to separations technologies,[6,7,15-19,20-24] while many natural systems and synthetic compounds tend towards formation of higher dimensional sheet topologies.[1] Less prevalent are structures consisting of infinite chains of cation-centered polyhedra, typically composed of uranyl centers bridged by tetrahedral linkages.[1,20,25] Herein, we report the synthesis and characterization of a novel monomeric species incorporating both, fully intact, ionic liquid moieties, with ligation by the anion $[C_5H_6N]_2$ $[UO_2(C_7H_7SO_3)_4(H_2O)]$ (**1**). We also report a compound that contains a zigzag chain of uranyl square bipyramids with a novel topology, $UO_2(HAsO_4)(NC_5H_{11}O_2)$ (**2**). These structures provide additional insight into the chemistry of the uranyl cation in protic-TSIL media.

Experimental

Synthetic procedures:

$UO_2(NO_3)_2{\cdot}6H_2O$ (MV Laboratories, Lot #s P705UA1, IBI55963), $UO_2(CH_3CO_2)_2{\cdot}2H_2O$ (MV Laboratories, Lot #s W105UA1), $MgSO_4{\cdot}7H_2O$ (Fisher Scientific 99.9%), $MgCl_2{\cdot}6H_2O$ (Fisher Scientific 99%), As_2O_5 (Aldrich 90%), $LiNO_3{\cdot}H_2O$ (Alfa Aesar 99%), Betaine HCl (Alfa Aesar 99%), $Li[(CF_3SO_2)_2N]^-$ (Alfa Aesar 98%) and pyridinium $[CH_3C_6H_4SO_3]^-$ (Alfa Aesar 98%) were

used as received. $UO_2(CF_3SO_3)_2$ was prepared in-house by reaction of UO_3 with triflic acid. The ionic liquid betainium bistriflimide ([HBet] [Tf_2N]) was prepared according to the method in the literature.[12] Ionothermal reactions were performed in 23 mL Teflon-lined stainless steel reaction vessels heated in mechanical convection ovens.

While isotopically depleted U was used in these experiments, precautions for handling radioactive materials should be followed.

$[C_5H_6N]_2$ $[UO_2(C_7H_7SO_3)_4(H_2O)]$ (**1**) was obtained by addition of 0.0439 g uranyl acetate, 0.0010 g magnesium chloride, and 0.3980 g pyridinium para-toluenesulfonate (PPTS) in a 1 : 0.05 : 16 molar ratio, respectively, along with a few drops of water to aid in solvation of PPTS into a test tube. Single crystals were retrieved after several weeks from slow evaporation. Yellow rectangular prisms of **1** were found in moderate yield (40% on the basis of uranium). Compound **1** was also synthesized using ionothermal methods (120 ºC for 4 days); however, this method yielded significant decomposition products and a lower yield of **1** (10% on the basis of uranium).

$UO_2(HAsO_4)(NC_5H_{11}O_2)$ (**2**) was obtained by addition of 2 mL of 0.1 M uranyl triflate, 0.0800 g arsenic pentoxide, and 0.0412 g lithium nitrate hydrate in a 2 : 3.5 : 5 molar ratio, respectively, followed by addition of 0.25 mL of betainium bistriflimide. The reaction vessel was placed in an oven at 120 ºC for five days, and was then removed and allowed to cool to ambient temperature. Two products were recovered by vacuum filtration. Millimeter sized greenish-yellow rectangular prisms of $LiUO_2(AsO_4)\cdot 4H_2O$[27] were produced in low yield (25% on the basis of uranium) and light-yellow needles of **2** were produced in a moderate yield (47% on the basis of uranium).

Alkali and alkali earth salts were added to the reactions to provide an alternative/competitive charge balance species for crystallization in lieu of the organic species, as was the case for the minor product $LiUO_2(AsO_4)\cdot 4H_2O$ in the synthesis of **2,** and to promote crystallization by increasing the solution ionic strength of the solutions.

Crystallographic Studies

Single crystals of **1** and **2** were selected, mounted on a cryoloop using viscous oil, and aligned on a Bruker three-circle X-ray diffractometer with an APEXII CCD area detector, using a graphite monochromated Mo*K*α microfocus sealed tube. A sphere of diffraction data was collected for each compound with 0.5° frame widths for **1** and 0.25° for **2** in ω and frame count times of 25 and 20 seconds per frame for **1** and **2,** respectively.

The Bruker APEX II software package was used to determine and refine unit-cell parameters using least-squares techniques and for data integration and corrections for background, Lorentz, and polarization effects.[28] SADABS was used to correct for absorption.[29]

Structure solutions and refinements were done using intrinsic phasing and the remaining atomic positions were located in difference-Fourier maps calculated subsequent to refinement of partial-structure models, using the Bruker SHELXTL software package.[30] The final refinements included anisotropic displacement parameters for all non-hydrogen atoms. Hydrogen associated with coordinated water O15 in **1** and coordinating hydroxyl O8 in **2** were neither located in difference-Fourier maps nor placed in calculated positions, and were therefore not included in the final refinement models. The OLEX2 software package was used in tandem with SHELXTL for modeling disorder and hydrogen position refinements. OLEX2 and CrystalMaker software packages were used to graphically model compounds.[31, 32]

Data collection parameters and crystallographic details are listed in *Table 1* and additional details are in the Supporting Information.

Table 1
Crystallographic data and refinement parameters

Formula	$[NC_5H_6]_2$ $[UO_2(C_7H_7SO_3)_4(H_2O)]$	$UO_2(HAsO_4)$ $(NC_5H_{11}O_2)$
CCDC	985929	985928
Formula mass	1133.00	521.11
Crystal system	Monoclinic	Monoclinic
Space group	$P2_1/c$	$P2_1/c$
a (Å)	12.392(2)	7.167(2)
b (Å)	36.745(4)	14.740(3)
c (Å)	10.246(1)	11.157(3)
β (°)	112.190(1)	96.747(4)
V (Å^3)	4319.7(9)	1167.6(4)
Z	4	4
λ (Å)	0.71073	0.71073
μ (mm^{-1})	4.020	16.740
θ (°) range	1.11 to 26.37	2.30 to 26.37
D_x (gm cm^{-3})	1.739	2.993
S	1.023	1.080
R(F) for $F_0^2 > 2\sigma(F_0^2)$ [a]	0.0328	0.0166
$R_w(F_0^2)$ [b]	0.0734	0.0381

[a] $R_1=\sum||F_0|-|F_c||/\sum|F_0|$.
GOOF =S=$\{\sum[w(F_0^2-F_0^2)^2]/(n-p)\}^{1/2}$.
[b] $wR_2=\{\sum[w(F_0^2-F_0^2)^2]/\sum[w(F_0^2)^2]\}^{1/2}$.
$W=1/\sigma(F_0^2)+(aP)^2+bP]$; where P is $[2F_c^2+\mathrm{Max}(F_0^2,0)]/3$

Spectroscopic Studies

Absorption spectra were obtained for neat crystalline samples at room temperature using a Craic Technologies UV−vis−near-IR (NIR) microspectrophotometer. The absorption data were collected over the range of 250-1200 nm.

X-ray fluorescence spectra were obtained for neat crystalline samples on carbon tape at room temperature, under vacuum, using an EDAX Orbis microXRF. Spectra were collected using 60 sec. collection times at 20 kV.

Infrared spectra were obtained for neat crystalline samples on a SensIR Technology IlluminatIR FT-IR microspectrometer. Samples were collected using a diamond ATR objective at room temperature with a beam aperture of 100 μm, over the range 650-4000 cm^{-1}.

Results

Crystal structures

The structural unit of **1** consists of a uranyl pentagonal bipyramid (Fig. 1). The two axial U-O "yl" bond lengths are 1.748(3) and 1.755(3) Å, and the O-U-O angle is 177.3(2)º. Four para-toluenesulfonate ligands, ligating through vertex sharing sulfonate polyhedra, and an H_2O group coordinate the uranyl ion in the equatorial plane of the resulting pentagonal bipyramid. The U-O_{eq} bond length ranges from 2.351(4) to 2.396(3) Å for the PTS ligands,

and is 2.493(3) Å for the water group. Whereas the anion constituent of the ionic liquid coordinates the uranyl center, the pyridinium cations provide for charge balance and form hydrogen bonding contacts with unbound sulfonate O atoms (2.004 and 2.069 Å). Likewise, the coordinated water also stabilizes the structure through hydrogen bonds that are accepted by sulfonate O atoms, as assigned between heteroatoms (O---O-S: 2.751 to 2.997 Å).

Figure 1: Thermal Ellipsoid plot showing the asymmetric unit of **1 (A)** and extended structure view showing H-bonding interactions (**B**)**.** For clarity, only pyridinium hydrogens involved in H-bonding are shown in **B**.

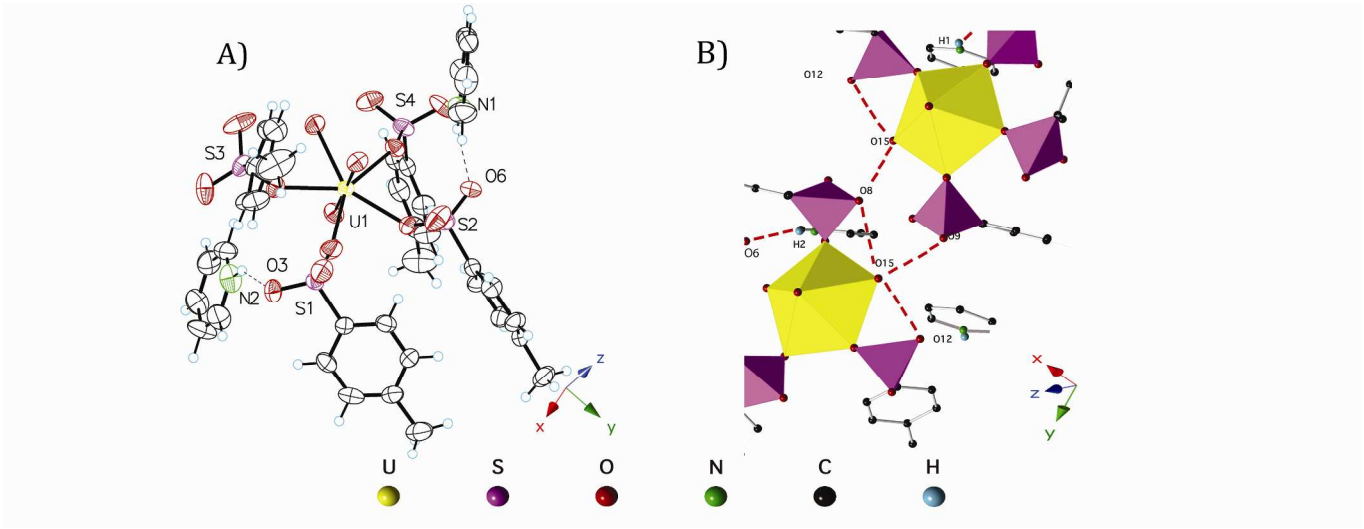

The structural unit of **2** consists of uranyl tetragonal bipyramids that are connected into a zigzag chain through corner-sharing with arsenate polyhedra through three equatorial sites, with a terminally coordinating betaine ligand at the fourth site (Fig. 2). The U-O bond lengths within the uranyl ion are 1.781(3) and 1.786(3) Å, and the O-U-O bond angle is 178.5(1)º. Isotropic modelling of the bridging arsenate O atoms gave U-O distances of 2.252(3) to 2.331(3) Å in the equatorial plane of the tetragonal bipyramid. The As-O bond lengths of bridging O atoms range from 1.70(3) to 1.73(3) Å. The presence of the non-bridging As-O bond length of 1.721(3) Å, and similar

Figure 2: Thermal Ellipsoid plot of the asymmetric unit (A), Mixed Polyhedra-Ball and Stick extended zigzag chain structure with hydrogens excluded (B), Alternate chain view along the y-axis with betaine hydrogens shown (C), and packing diagram (D) of compound **2**.

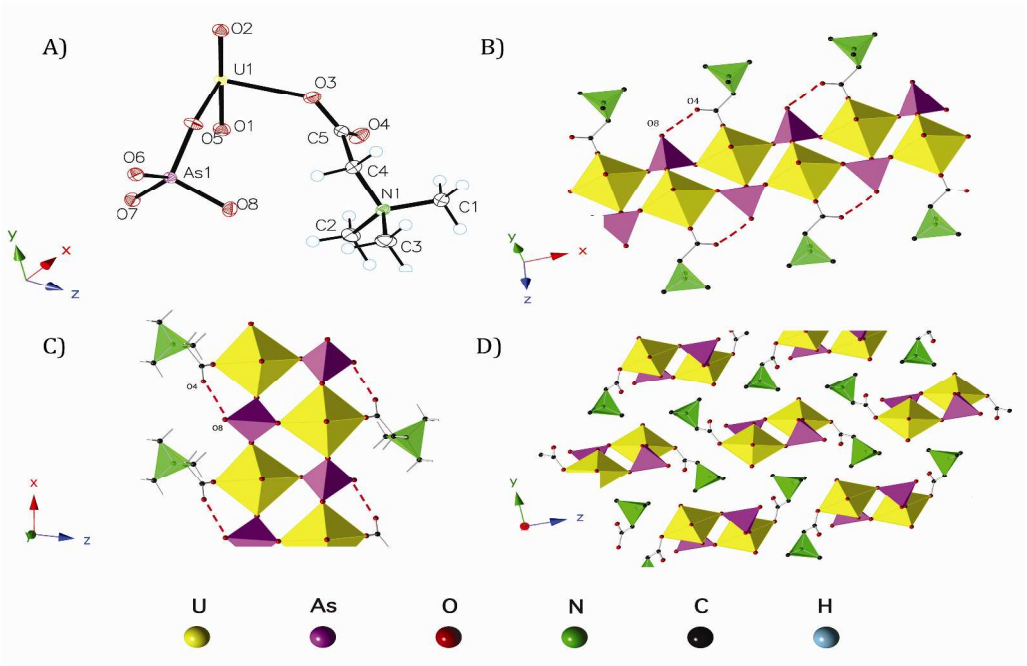

bond lengths for the carboxyl O atoms of the betaine 1.237(5) (non-bridging) and 1.279(5) Å (bridging), allows for designation of a non-bridging arsenate hydroxyl group. Therefore, a hydrogen bonding contact may be assigned (2.613 Å) between heteroatoms of the non-bridging oxygen, As-O(8) and the non-bridging O(4) of the carboxyl moiety. This gives a neutral zigzag uranyl-arsenate chain ligated by the neutral betaine zwitterion. Additional interatomic distances can be found in Table 2, while hydrogen bonding distances for the two compounds are located in Table 3.

Table 2
Select interatomic distances (Å)

Compound **1**		Compound **2**	
$U\text{-}O_{13}$	1.748(3)	$U\text{-}O_1$	1.786(3)
$U\text{-}O_{14}$	1.755(3)	$U\text{-}O_2$	1.781(3)
$U\text{-}O_1$	2.351(4)	$U\text{-}O_3$	2.331(3)
$U\text{-}O_4$	2.371(3)	$U\text{-}O_5$	2.259(3)
$U\text{-}O_7$	2.357(3)	$U\text{-}O_6$	2.252(3)
$U\text{-}O_{10}$	2.396(3)	$U\text{-}O_7$	2.286(3)
$U\text{-}O_{15}$	2.493(3)	$As\text{-}O_5$	1.670(3)
$S\text{-}O_{Coord.}$ (Avg.)	1.480	$As\text{-}O_6$	1.673(3)
$S\text{-}O_{UnCoord.}$ (Avg.)	1.439	$As\text{-}O_7$	1.670(3)
N-C (Avg.)	1.322	$As\text{-}O_8$	1.721(3)
$C\text{-}C_{pyr.}$ (Avg.)	1.353	$C_5\text{-}O_3$	1.279(5)
		$C_5\text{-}O_4$	1.237(5)
(I) x, -y+1/2, z-1/2		(I) x-1, y, z	
(II) x, -y+1/2, z+1/2		(II) -x+1, -y+1, -z+1	
		(III) x+1, y, z	

Table 3
Hydrogen bonding distances (Å)

Compound **1**		Compound **2**	
$N_1\text{-}H_1\cdots O_{11}$	2.004(3)	$As\text{-}O_8H\cdots O_4$	2.613(5)
$N_2\text{-}H_2\cdots O_8$	2.069(3)		
$O_{15}\text{-}H\cdots O_{12}$	2.751(3)		
$O_{15}\text{-}H\cdots O_{9'}$	2.884(3)		
$O_{15}\text{-}H\cdots O_8$	2.997(3)		

UV-vis-NIR Spectroscopy

The UV-vis-NIR spectrum for each compound displays the characteristic fine structure of the vibronically coupled uranyl absorption bands, centered around 413 – 425nm. Also present are the characteristic broad LMCT bands centered around 300-330nm.[33 34] Individual spectra are provided in the Supporting Information.

X-ray Fluorescence Spectroscopy

Elemental analysis for elements heavier than Na was performed and confirmed the crystallographically determined ratios of uranium and sulfur (**1**) or arsenic (**2**). Full energy dispersive spectra are provided in the Supporting Information.

ATR-FTIR Spectroscopy

Infrared spectra confirmed the presence of U(VI) by revealing the characteristic ν_3 antisymmetric vibrational mode of the uranyl ion (933 and 901cm^{-1} respectively). Individual spectra are provided in the Supporting Information.

The infrared spectrum of **1** (Fig. 3) contains absorption bands: 676s, 707w, 745m, 814m, 849w, 875w, 933m, 991s, 1027m, 1101s, 1125s, 1153m, 1180m, 1239m, 1379w, 1427w, 1455wm 1483w, 1535w, 1606w, 1636w, 1707w, 2882w, 3072m:br, 3175w, confirming the presence of pyridinium and para-toluenesulfonate moieties in addition to the aforementioned uranyl stretching mode.

The infrared spectrum of **2** (Fig. 4) contains absorption bands: 697m, 760s, 801s, 834s, 866s, 901m, 928m, 955w, 989w, 1129w, 1209w, 1241w, 1315s, 1328m, 1401m, 1423m, 1442m, 1459m, 1477m, 1494m, 1634m, 1641m, 1980w, 2344m, 2359m, 2849m,br, 2992w, 3044w, 3061w, confirming the presence of both betainium and arsenate with a sharp As-O-M vibrational band at 760 cm^{-1}, strong $HAsO_4$ symmetric stretching bands at 801 and 834 cm^{-1}, an antisymmetric band at 866 cm^{-1}, and hydroxyl stretches at 1634 and 1641 cm^{-1}.[34, 35] Assignment of the antisymmetric uranyl stretching vibration remains ambiguous for this spectrum due to strong overlapping bands between $HAsO_4$ and betaine in the 800-1000 cm^{-1} region.

Figure 3: UV-vis-NIR spectra of **1** and **2**.

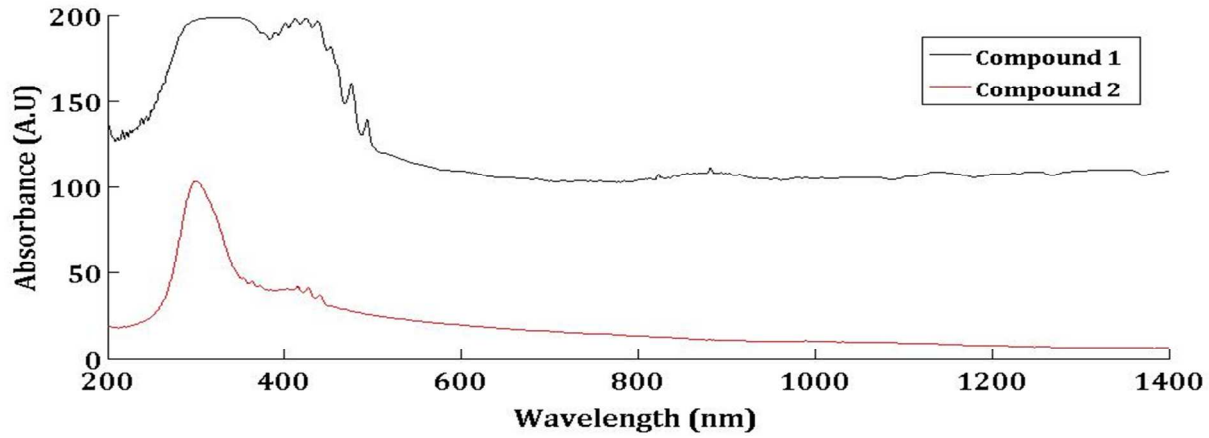

Figure 4: Infrared spectra of **1** and **2** over the range of 650 to 4000 cm^{-1}.

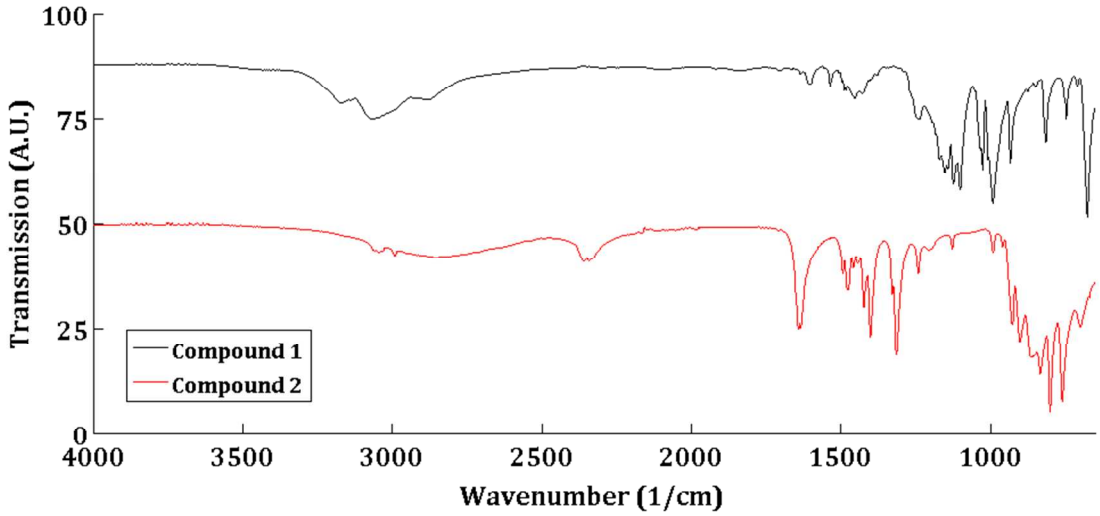

Discussion

The use of task specific ionic liquids as both solvent and reagent provides a unique avenue for probing uranyl chemistry in the absence of excess water. It is our goal to utilize TSILs in our investigations of the interplay between coordinating ligands, charge-balancing species, and how the TSILs affect overall dimensionality as compared to conventional hydrothermal methods.

Whereas examples are known of monomeric uranyl species coordinated by the O-donor ligand of a solvating ionic liquid, compound **1** is of interest in that the coordinating species is anionic. Typically coordination occurs via deprotonated carboxyl group(s) or similar species, yielding a neutral ligand, or by moiety degradation to yield an anionic ligand. Also present in the compound is the intact cationic moiety, which provides charge balance and hydrogen bonding contacts for structural stability. To our knowledge, this compound is the first uranyl compound that has incorporated both, fully intact, IL moieties, wherein the anion is coordinating PTS and there is charge-balancing pyridinium.

Compound **2**, of higher dimensionality, is essentially an auxiliary product of $LiUO_2AsO_4{\cdot}4H_2O$[27] terminated by the neutral betaine zwitterion, thus preventing the structural unit from extending into a corrugated sheet topology as occurs in $LiUO_2AsO_4{\cdot}4H_2O$. Instead, the terminal betaine promotes the formation of the zigzag chain.

The uranyl coordination in **2** is tetragonal bipyramidal with three coordinating monodentate arsenate tetrahedra. Each arsenate is coordinated to three uranyl centers: two provide the linkages that form the linear component of the chain, and one is normal to the chain direction. The non-bridging arsenate oxygen is designated as hydroxyl in lieu of protonation at the betainium on the basis of bond length measurements (As-O_8 is 0.050 Å longer than As–$O_{bonding\ avg}$ and the 0.042 Å shorter double bond of the carbonyl C_5-O_4 over the elongated bridging C_5-O_3) and the Ka's of arsenate ($K_{a3} = 10^{-11.5}$) and betainium ($K_a = 10^{-1.83}$). The hydroxyl projects outward from the chain, perpendicular to the chain direction, and forms a hydrogen bond with the uncoordinated oxygen on the betaine carboxyl group.

Amino acids and their derivatives have been used to great effect in the past to coordinate uranyl species.[12,16,20,25] The main applications have been in separations and solution studies. As such, little is known about how these species behave in more complex systems or in the solid state. Deprotonation of betainium to form the betaine zwitterion is consistent with typical ionothermal reaction products in the literature. Note that the carboxyl group is monodentate. The strong hydrogen bonding interactions, uranyl's high affinity towards arsenates, and steric considerations associated with the betaine moiety, directed the formation of the tetragonal bipyramid instead of the more common pentagonal or hexagonal bipyramid species.

The structural motif in **2** appears to be novel within uranyl topologies, owing to the tetragonal bipyramidal arrangement of the uranyl ion.

The effect of ionothermal methods as compared to slow evaporation of ILs is notable here. Slow evaporation of the IL resulted in a higher product yield of **1**, as a consequence of lack of reaction below 100 ºC and partial thermal decomposition at temperatures approaching the melting point of the ionic liquid at 120 ºC by ionothermal methods. Conversely, compound **2** was synthesized using ionothermal methods, whereas changing the synthesis method to slow evaporation yields the uranyl arsenate chain structure $UO_2(H_2AsO_4)_2(H_2O)$.[36] Lack of thermal energy allows for phase separation and exclusion of betaine from the reaction.

Conclusions

In this study we report the synthesis of two novel uranyl coordination compounds derived from syntheses using

betainium and pyridinium class ionic liquids. This work demonstrates the importance of further developing the understanding of uranyl chemistry outside of conventional hydrothermal methods, as it further illustrates the importance of probing H-bonding interactions and their roles in directing/stabilizing the various uranyl topologies. Valuable insight has been gained into synthetic strategies for promoting desired complexities, and future research will build on these foundations for the development of a better toolbox of synthetic techniques for engineering novel actinyl compounds.

Acknowledgements

This research was supported by the Chemical Sciences, Geosciences and Biosciences Division, Office of Basic Energy Science, Office of Science, U.S. Department of Energy, Grant No. DE-FG02-07ER15880.

EDAX analyses were conducted at the Center for Environmental Science and Technology at the University of Notre Dame.

Notes and references

[a] Department of Civil and Environmental Engineering and Earth Sciences, University of Notre Dame, Notre Dame, IN 46556, USA
[b] Department of Chemistry and Biochemistry, University of Notre Dame, Notre Dame, IN 46556, USA

Electronic Supporting Information (ESI) available: [UV-vis-NIR, ATR-FTIR, and XRF EDAX spectra, additional structural figures for **1** and **2,** and crystallographic parameters].

CCDC 985929 and 985928 contain the supplementary crystallographic data for **1** and **2**, respectively. These data can be obtained at no cost via www.ccdc.cam.ac.uk/data_request/cif, by e−mailing data_request@ccdc.cam.ac.uk, or by contacting The Cambridge Crystallographic Data Centre 12 Union Road Cambridge CB2 1EZ, UK, Fax: +44(0)1223−336033. See DOI: 10.1039/c000000x/

1 P. Burns, *Can. Mineral*., 2005, **43**, 1839.
2 S. Liu, M. Chen, B. Chang, and K. Lii, *Inorg. Chem.,* 2013, **52**, 3990.
3 J. D. Woodward, T. E. Albrech-Schmitt, *J. Solid State Chem.*, 2005, **178**, 2922.
4 E. M. Wylie, M. K. Dustin, J. S. Smith, and P. C. Burns, *J. Solid State Chem.,* 2013, **197**, 266.
5 P. Wasserscheid and T. Welton, Eds., *Ionic Liquids in Synthesis,* Wiley- VCH Verlag GmbH & Co. KGaA, Weinheim, 2nd edn, 2008, vol. 1–2.
6 P. S. Barber, S. P. Kelley, and R. D. Rogers, *RSC Advances*, 2012, **2**, 8526.
7 X. Chen, G. S. Goff, M. Quiroz-Guzman, D. P. Fagnant Jr., J. F. Brennecke, B. L. Scott, and W. Runde, *Chem. Commun., 2013,* **49**, 1903.
8 E. R. Parnham, R. E. Morris, *Acc. Chem. Res*., 2007, **40**, 1005.
9 R. E. Morris, Angew. *Chem. Int. Ed*., 2008, **47**, 442.
10 P. S. Wheatley, P. K. Allan, S. J. Teat, S. E. Ashbrook, and R. E. Morris, *Chem. Sci.,* 2010, **1**, 483.
11 D. S. Wragg, A. M. Z. Slawin, and R. E. Morris, *Solid State Sci*., 2009, **11**, 411.
12 P. Nockemann, B. Thijs, S. Pittois, J. Thoen, C. Glorieux, K. Van Hecke, L. Van Meervelt, B. Kirchner, and K. Binnemans, *J. Phys. Chem. B*, 2006, **110**, 20978.
13 P. Nockemann, B. Thijs, K. Van Hecke, L. Van Meervelt, and K. Binnemans, *Cryst. Growth Des*., 2008, **8**, 1353.
14 J. H. Davis Jr., *Chem. Letters*, 2004, **33**, No. 9, 1072.
15 V. Cocalia, K. Gutowski, and R. Rogers, *Coord. Chem. Rev*., 2006, **250**, 755.
16 C. J. Rao, K. A. Venkatesan, K. Nagarajan and T. G. Srinivasan, *Radiochim. Acta.,* 2008, **96**, 403.
17 A. Rout, K. A. Ventatesan, T. G. Srinivasan, and P.R. Vasudeva Rao, *J. Haz. Mat.* 2012, **221-222**, 62.
18 K. Takao, T. J. Bell, and Y. Ikeda, *Inorg. Chem.*, 2012, **52**, 3459.
19 V. Cocalia, M. Smiglak, S. T. Kelley, J. L. Shamshina, G. Gurau, and R. D. Rogers, *Eur. J. Inorg. Chem*., 2010, 2760.
20 P. Nockemann, R. Van Deun, B. Thijs, D. Huys, E. Vanecht, K. Van Hecke, L. Van Meervelt, and K. Binnemans*, Inorg. Chem*., 2010, 49, 3351.
21 K. Servaes, C. Hennig, I. Billard, C. Gaillard, K. Binnemans, C. Gorller-Walrand, and R. Van Deun, *Eur. J. Inorg. Chem*., 2007, **32**, 5120.
22 A. E. Bradley, J. E. Hatter, M. Nieuwenhuyzen, W. R. Pitner, K. R. Seddon, and R. C. Thied, *Inorg. Chem.,* 2002, **41**, 1692.
23 A. S. Lermontov, E. K. Lermontova, and Y. Wang, *Inorg. Chim. Acta,* 2009, **362**, 3751.
24 M. Sornein, M. Mendes, C. Cannes, C. Le Naour, P. Nockemann, K. Van Hecke, L. Van Meervelt, J. Berthet, and C. Hennig, *Polyhedron*, 2009, **28**, 1281.
25 J. de Groot, K. A. Gojadas, D. K. Unruh, T. Z. Forbes, *246th Natl. Meet. Am. Chem. Soc., Div. Nuc. Chem.* 2013, NUCL 22.
26 T. G. Parker and T. E. Albrecht-Schmitt, *Cryst. Growth and Design*, 2014, **14**(1), 228.
27 A. N. Fitch, B. E. F. Fender, and A. F. Wright, *Acta Cryst,* 1982, **B38**, 1108.
28 Bruker, APEX2 v2010, Bruker AXS Inc., Madison, WI, 2010.
29 G.M. Sheldrick, R.H. Blessing, Acta Crystallogr. A51 (1995) 33.
30 G.M. Sheldrick, Acta Cryst. A**64** (2008), 112.
31 O. V. Dolomanov, L. J. Bourhis, R. J. Gildea, J. A. K. Howard, and H. Puschmann, "OLEX2: a complete structure solution, refinement and analysis program". J. Appl. Cryst. 2009, **42**,339.
32 CrystalMaker: a crystal and molecular structures program for Mac and Windows. CrystalMaker Software Ltd, Oxford, England (www.crystalmaker.com)
33 L. R. Morss, N. M. Edelstein, and J. Fujer, Eds, *The Chemistry of the Actinide and Transactinide Elements*, Springer, The Netherlands, 2006, Vol. 3-**4**
34 P. C. Burns and R. Finch, Eds., *Reviews in Mineralogy,* 1999, **38**.
35 S. C. B. Myneni, S. J. Traina, G. A. Waychunas, and T. J. Logan, *Geochemica et Cosmochimica Acta*, 1998, **62**, No. 21/22, 3499.
36 T. Geising and C.H. Rüscher, *Z. Anorg. Allg. Chem.* 2000, **626**, 1414

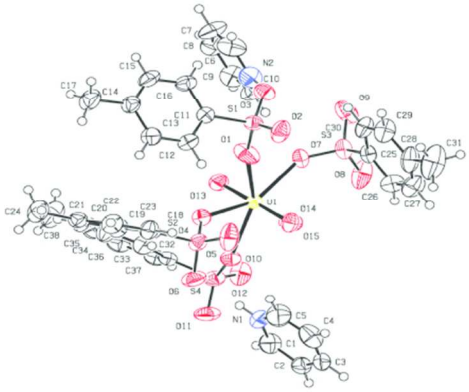

$[C_5H_6N]_2[UO_2(C_7H_7SO_3)_4(H_2O)]$

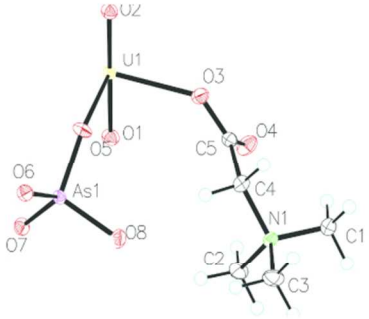

$UO_2(HAsO_4)(NC_5H_{11}O_2)$

80x40mm (300 x 300 DPI)

Task Specific Ionic Liquids are employed in the development of two new low-dimensionality uranyl compounds.